Selective Inhibition of Trypsins by Insect Peptides: Role of P6−P10 Loop

C. Kellenberger,*,‡ G. Ferrat,§ P. Leone,§ H. Darbon,§ and A. Roussel*,§

Centre d'Immunologie de Marseille-Luminy, UMR 145, Parc Scientifique et Technologique de Luminy, Case 906, 13009 Marseille, France, and Architecture et Fonction des Macromolécules Biologiques, UMR 6098 Centre Nationale de la Recherche Scientifique, 31 chemin J. Aiguier, 13402 Marseille Cedex 20, France

Received July 24, 2003; Revised Manuscript Received September 25, 2003

ABSTRACT: PMP-D2 and HI, two peptides from *Locusta migratoria*, were shown to belong to the family of tight-binding protease inhibitors. However, they interact weakly with bovine trypsin (K_i around 100 nM) despite a trypsin-specific Arg at the primary specificity site P1. Here we demonstrate that they are potent inhibitors of midgut trypsins isolated from the same insect and of a fungal trypsin from *Fusarium oxysporum* ($K_i \leq 0.02$ nM). Therefore, they display a selectivity not existing for the parent chymotrypsin inhibitor PMP-C. By NMR, we demonstrate that HI possesses a highly rigid structure similar to the crystal structure of a variant of PMP-D2 in complex with bovine α-chymotrypsin. The main difference with PMP-C is located in the region from residues 20 to 24 (positions P6−P10) that interacts with the loop containing Gly173 in chymotrypsin. The corresponding residue in mammalian trypsins is always a proline that may generate a steric clash with the inhibitor. The residues thought to confer selectivity were mutated with PMP-C as a model. The resulting analogue PMP-D2(K10W,P21A,W25A) loses some activity toward insect and fungal trypsins but is a more potent inhibitor of mammalian trypsins, corresponding to a decrease of selectivity. This work represents a first attempt in tuning the selectivity of natural peptidic serine protease inhibitors by mutating residues out of the reactive loop (P3−P′3).

During the last two decades, a large number of serine protease inhibitors have been characterized, ranging from microorganisms to mammals (*2*). In particular, trypsin and α-chymotrypsin inhibitors have been reported in the hemolymph of a wide range of arthropods and insects (*3*). Most of these inhibitors fall into established families such as Kazal, Kunitz, Ascaris, or serpins.

In this context, one novel family has emerged, with detailed biochemical and structural studies of peptidic inhibitors isolated from the grasshoppers *Locusta migratoria* and *Schistocerca gregaria* (*4*, *5*). These peptides were named PMP-C, PMP-D2 and HI for *L. migratoria* and SGCI and SGTI for *S. gregaria*. As illustrated in Figure 1A, PMP-C and SGCI present 85% sequence identity while PMP-D2, HI, and SGTI are 70−80% homologous. They are 35−36 residues long with six cysteines involved in three disulfide bonds. We previously showed that PMP-C is a very potent inhibitor of bovine α-chymotrypsin ($K_i = 0.13$ nM) while PMP-D2 and HI are only weak inhibitors ($K_i = 1500$ nM and 340 nM, respectively). The P1 residue in the reactive site, which is the primary determinant for the enzyme specificity [nomenclature according to Schechter and Berger (*1*)],[1] was determined to be Leu30 for PMP-C and Arg29 for PMP-D2 and HI. One unique mutation at P1 position (Arg to Leu) converts PMP-D2 and HI into potent bovine α-chymotrypsin inhibitors (*4*). Strikingly, PMP-D2 and HI fail to inhibit porcine trypsin although they bear a favorable

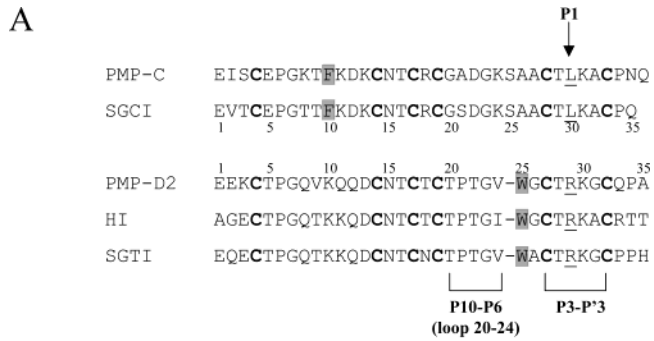

FIGURE 1: Sequences of the members of the grasshopper family. (A) Alignment of PMP-C, SGCI, PMP-D2, HI, and SGTI. A gap is introduced to optimize alignment. The P1 residue is underlined. The cysteines are in boldface type. The aromatic residues are shaded in gray. (B) Sequences of analogues derived from PMP-D2. The mutated residues are shaded in gray.

P1 residue (Arg). In the same manner, SGTI is a weak inhibitor of bovine trypsin while SGCI inhibits strongly bovine chymotrypsin and can be converted to a potent trypsin inhibitor by mutating P1−P′1 residues. All these data indicate differences in the inhibitory properties between the trypsin inhibitors (PMP-D2, HI, and SGTI) and chymotrypsin inhibitors (PMP-C and SGCI) among the grasshopper family.

The tertiary structures of PMP-C, PMP-D2, SGCI, and SGTI were determined by NMR (*6*−*8*). They consist of a twisted β-sheet, composed of three antiparallel strands, stabilized by three disulfide bonds. In addition, we solved

* Corresponding authors: kellenberger@ciml.univ-mrs.fr and roussel@afmb.cnrs-mrs.fr.

‡ Centre d'Immunologie de Marseille-Luminy, UMR 145.

§ Architecture et Fonction des Macromolécules Biologiques, UMR 6098.

10.1021/bi035318t CCC: $25.00
Published on Web 11/01/2003

the crystal structures of PMP-C and of an analogue of PMP-D2 (PMP-D2v), in complex with bovine α-chymotrypsin (*9*). This study highlighted structural divergences between the two inhibitors that result in an additional interaction site for PMP-D2v.

In the present report, we determined the solution structure of HI by NMR. We also show that PMP-D2 and HI are very potent inhibitors of digestive trypsins from *Locusta migratoria*. We thus predict these proteases to be some of their physiological targets. Contrarily to the chymotrypsin inhibitors of the grasshopper family, the trypsin inhibitors display a high degree of selectivity. This phenomenon has rarely been studied for peptidic inhibitors, while huge efforts have been made to understand and improve specificity of small organic compounds. In that case, the differential activities are based upon subtle differences in the S1 site of the enzyme (for an example, see ref *10*) but such mechanisms cannot be exploited by natural peptidic inhibitors. Indeed the sequence of the active loop (P3−P′3) is highly conserved among the family, except for the P1 residue. Therefore the structural features of discrimination displayed by PMP-D2 and HI have to be investigated out of the active loop. Using data generated from crystal and NMR structures together with structure-guided analogues, we highlight the possible role of the secondary interaction site at position P6−P10.

EXPERIMENTAL PROCEDURES

Materials. The Fmoc amino acids derivatives, BOP, and Wang resins were obtained from Neosystem and Novabiochem. The porcine and bovine trypsins were obtained from Sigma. The substrate Bz-DL-Arg-pNa (BApNa), was from Bachem, and Bz-Ile-Glu-Gly-Arg-pNa (S-2222) and pyro-Glu-Gly-Arg-pNa (S-2444) were from Chromogenix. BPTI was purchased from Biosys.

TRY1 and TRY2A were kindly provided by W. Lam and colleagues, in 50 mM Tris-HCl buffer, pH 8, and 10 mM $CaCl_2$; TRY2A also contained 500 mM NaCl. The active enzymes were titrated with PMP-D2 or HI, as described below. *Fusarium oxysporum* trypsin was a gift from Dr W. Rypniewski. It was kept inhibited in a buffer containing 100 mM boric acid, 2 mM $CaCl_2$, 100 mM NaCl, and 100 mM 3,3-dimethylglutaric acid, pH 6.

Synthesis of Peptides. The syntheses of PMP-D2 and HI were previously described (*4*). The analogues PMP-D2(13−35), PMP-D2(C17H/C27S), and PMP-D2(K10W/P21A/W25A) were synthesized on an Advanced ChemTech 90 (ACT 90) synthesizer, via Fmoc strategy, starting with WANG substituted resins. The side-chain protecting groups were the following: Boc for Lys and Trp; *t*-Bu for Asp, Glu, and Thr; Pmc for Arg; and Trt for Asn, Gln, and Cys. The coupling reactions were achieved in DMF by use of 3−5 equiv of protected amino acid, 3−5 equiv of BOP, and 12−20 equiv of DIEA. The deprotection reactions were made with 25% piperidine in DMF. The cleavage of the peptide from the resin (150−200 mg) was done in 10 mL of TFA/0.75 g of phenol/0.5 mL of water/0.75 mL of TIS for 1.5−2 h. The crude peptide was recovered by filtration, washed three times with methyl *tert*-butyl ether, solubilized in 10% AcOH, and lyophilized. The crude peptides were air-oxidized at 1−2 mg/mL concentration either in water at pH adjusted to 8 or in a 0.1 M Tris buffer, pH 8. Before purification, the oxidized peptides were acidified with TFA. The mixtures were then directly loaded onto preparative and semipreparative columns (Vydac C18 and aquapore C8) and eluted with a stepwise gradient. The peptides were characterized by mass spectrometry.

Serine Protease Inhibition. All the experiments were done in triplicate in buffers containing 100 mM Tris buffer at pH 8, plus 100 mM NaCl for bovine, porcine, and locust trypsins at 25 °C. For *Fusarium oxysporum*, enzyme and inhibitor were incubated in diluted HCl at pH 4, and to start the reaction the pH was increased to 8 by adding 0.95 M Tris buffer, pH 8, and 100 mM $CaCl_2$. The concentrations of bovine trypsin and inhibitors were determined from their optical density at 280 nm. The concentrations of active locust and fungal trypsins were estimated by titration with locust peptides (HI or PMP-D2).

In a first set of experiments, trypsins were used at a concentration between 30 and 100 nM, with BApNa as the substrate. The K_m constants were determined as $K_m = V_{max}/2$ by incubating increasing amounts of substrate to a constant amount of enzyme and measuring the release of *p*-nitroaniline (pNa) at 405 nm. The K_m values are 2.0 ± 0.2 mM (bovine), 0.27 ± 0.06 mM (locust TRY1), 0.075 ± 0.01 mM (locust TRY2A), and 0.12 ± 0.02 mM (fungal trypsin). In a second set of experiments, lower concentrations of locust trypsin TRY1 were used (3−4 nM) together with more sensitive substrates, S-2444 or S-2222. Their K_m for TRY1 was calculated to be 0.1 ± 0.01 and 0.029 ± 0.006 mM, respectively. For low concentrations of TRY2A, no appropriate conditions could be found with such a sensitive substrate.

Determination of Equilibrium Dissociation Constants. Constant concentrations of enzyme (30−100 nM or 2−3 nM range) and increasing concentrations of inhibitor were incubated for 30 min at room temperature. The reaction was started by adding specific substrate (5−10 μL), either BApNa or S-2222, and followed for 4 min at 405 nm. The results were interpreted as described by Bieth (*11*). The true K_i was calculated from K_{iapp} by use of the equation $K_i = K_{iapp}/(1 + S_0/K_m)$.

Determination of Association Rate Constants K_{assn}. The association rate constant K_{assn} was measured under second-order conditions. Equal concentrations of enzyme and inhibitor (at nanomolar range) were incubated for variable periods of time (from 30 s to 30 min). The reaction was started by addition of substrate S-2222 (5−10 μL), which slows the association process enough to measure the fractional activity and the release of pNa was monitored at 405 nm. The results were expressed as fractional activity (*a*) versus incubation time (*t*). The incubation time that

[1] Abbreviations: BPTI, bovine pancreatic trypsin inhibitor; Bz-DL-Arg-pNa, benzoyl-DL-arginine *p*-nitroanilide; FMOC, 9-fluorenylmethoxycarbonyl; BOC, butyloxycarbonyl; tBu, *tert*-butyl; Pmc, 2,2,5,7,8-pentamethylchroman-6-sulfonyl; Trt, trityl; DMF, dimethylformamide; BOP, benzotriazol-1-yloxytris(dimethylamino)phosphonium hexafluorophosphate; DIEA, diisopropylethylamine; TFA, trifluoroacetic acid; TIS, triisopropylsilane; AcOH, acetic acid; DQF-COSY, 2D double-quantum-filtered correlation spectroscopy; TOCSY, total correlation spectroscopy; NOESY, two-dimensional nuclear Overhauser effect spectroscopy; nOe, nuclear Overhauser effect; RMSD, root-mean-square deviation. The Schechter−Berger (*1*) nomenclature is used to specify residue positions relative to the reactive-site peptide bond (P1 is the residue whose side chain is recognized by the specificity pocket S1 of the proteinase; residues P*n* are to the N-terminal side of the cleavage site; residues P′*n* are to the C-terminal side).

produces a fractional activity of 0.5 ($=t_{1/2}$) was graphically deduced and K_{assn} was estimated from the equation $K_{assn} = 1/(E_0 t_{1/2})$.

Circular Dichroism. CD spectra were recorded on a Jasco spectrometer by accumulating three scans obtained with an integration time of 2 s and sampling points every 0.4 nm. Baseline spectra were subtracted from each spectrum. Peptide concentration (in water) was about 5×10^{-5} M, as determined by use of extinction coefficients of 260 M^{-1} cm^{-1} for PMP-C and 5500 $M^{-1}cm^{-1}$ for HI, PMP-D2, and its variants. The path length of the cell was 0.1 cm and the molar ellipticity was expressed in degrees centimeter^2 decimole^{-1}.

NMR Study: (*A*) *^{1}H NMR Spectroscopy*. HI was dissolved in 0.5 mL of H_2O/D_2O (90:10 v/v), pH 3, uncorrected for isotope effects. The amide proton exchange rate was determined after lyophilization and dissolution in 100% D_2O. All ^{1}H NMR experiments were performed on a Bruker DRX500 spectrometer equipped with a proton/carbon/nitrogen probe and self-shielded triple axis gradients. All spectra were recorded at 290 K: one DQF-COSY and one TOCSY spectrum for spin system identification and two NOESY spectra with mixing time values of 80 and 150 ms for sequential assignment and nOe collection.

(*B*) *Data Processing*. Spectra were processed with Bruker UXNMR software and analyzed with the XEASY software (*12*). The identification of the amino acid spin systems and the sequential assignment were performed by using the standard strategy described by Wüthrich (*13*). The nOe data were integrated with the manual procedure of XEASY for NOESY spectra. Distance geometry calculations were performed with the DIANA 2.8 software (*14*), as previously described (*15*). The values of α torsion angle constraints were obtained via coupling constant measurement on the DQF-COSY spectrum. The $^3J_{HN\alpha}$ coupling constant was translated into −40°/−70° and −70°/170° angle restraints, corresponding respectively to small (<7 Hz) and large (>8 Hz) coupling constants. The visual analysis of the quality of the structures was done with the Turbo-Frodo software (*16*). The exchange rate of amide protons with the solvent (D_2O) was measured. Amide protons that were still present after 30 h of exchange were considered as being involved in hydrogen bonds. Quantitative analysis was realized with PROCHECK-NMR (*17*).

RESULTS

Structure of HI in Solution. Structural studies have been completed on several members of the grasshopper family. The structures of PMP-C (*7*), PMP-D2 (*6*), and SGCI and SGTI (*8*) have been solved by NMR. In addition, PMP-C and PMP-D2 were further characterized at the atomic level in complex with bovine chymotrypsin (*9*). Moreover, the coordinates of PMP-D2 have not been deposited within the Protein Data Bank and the structure of HI has not been investigated yet. We have therefore undertaken an NMR study on this peptide. The structure was calculated by means of proton−proton distances derived from nOes and hydrogen bonds and by means of angle restraints derived from coupling constant values. The resulting single family of solutions showed neither distance violations >0.2 Å nor angle violations >5°. The repartition of nOes in different classes as well as the structural statistics for the 16 best solutions are given in Table 1.

Table 1: Calculation Statistics for the 16 Best Solution Structures of HI

distance constraints	
intraresidue/sequential nOes	303
medium-range nOes	16
long-range nOes	87
total nOes	406
hydrogen bonds	20
angle restraints	18
total constraints	444 (12.8 per residue)

	RMSD for backbone (Å)	RMSD for non-hydrogen atoms (Å)
overall	1.98 (± 0.51)	2.97 (± 0.60)
residues 3−28	0.62 (± 0.20)	1.25 (± 0.29)

The peptide is formed of one β-sheet made of three antiparallel strands (residues 8−12, 15−19, and 25−27) that are connected by one turn (residues 12−15) and one loop (residues 20−24). The N- and C-terminal extremities (residues 1−7 and 30−35) are very exposed to the solvent and are not stabilized in the solution structure. The main difference between solution structures of HI and PMP-D2 is the stability of the loop 20−24. In the description of PMP-D2, the authors pinpointed that this loop was not well defined due to the lack of nOes in this region. Furthermore, a dynamic study described slow movements of this loop on the time scale of micro- to milliseconds (*18*). However, in the loop 20−24 of HI, a large number of nOes (including long range) have been collected, leading to 21.6 nOes per residue on the average, far over the overall value, implying that there is a rigid conformation (see Supporting Information, Figure 1). In addition, Trp25 is highly constrained by long-range nOes involving the 8−12 strand, especially Lys10 (Figure 2A). This strong interaction locks the overall conformation of the loop 20−24 (Figure 2B).

Inhibition of Bovine and Locust Trypsins by Locust Peptides PMP-D2 and HI. Inhibition experiments show that HI and PMP-D2 are rather weak bovine trypsin inhibitors with K_i values of about 40 and 100 nM, respectively (Table 2). These results are in accordance with the activity of *S. gregaria* trypsin inhibitor (SGTI) recently published (K_i = 200 nM) (*5*). SGTI, which was isolated from testis and ovaries of the gregarious grasshopper *S. gregaria*, displays 77% identity with PMP-D2, with an arginine residue at P1 position.

Recently, several isoforms of trypsins (cationic and anionic) were isolated in midgut preparations from *L. migratoria* by Lam et al. (*19*). In this study the authors reported their catalytic properties together with their N-terminal sequences (11 residues). Here we assay the sensitivity of two chromatographically homogeneous proteases TRY1 (cationic) and TRY2A (anionic) toward PMP-D2 and HI, and the well-characterized bovine pancreatic trypsin inhibitor, BPTI (Table 2). PMP-D2 and HI are potent inhibitors of cationic locust trypsin TRY1 ($K_i \leq 0.02$ nM) as suggested by the linear inhibition curves of TRY1 (Supporting Information, Figure 2A). The association constants of PMP-D2 and HI were evaluated under second-order conditions to be $K_{assn} = (1.5 \pm 0.5) \times 10^6$ M^{-1} s^{-1} (Supporting Information, Figure 2B) and $K_{assn} \geq (7 \pm 1.5) \times 10^6$ M^{-1} s^{-1}, respectively. BPTI is a rather moderate

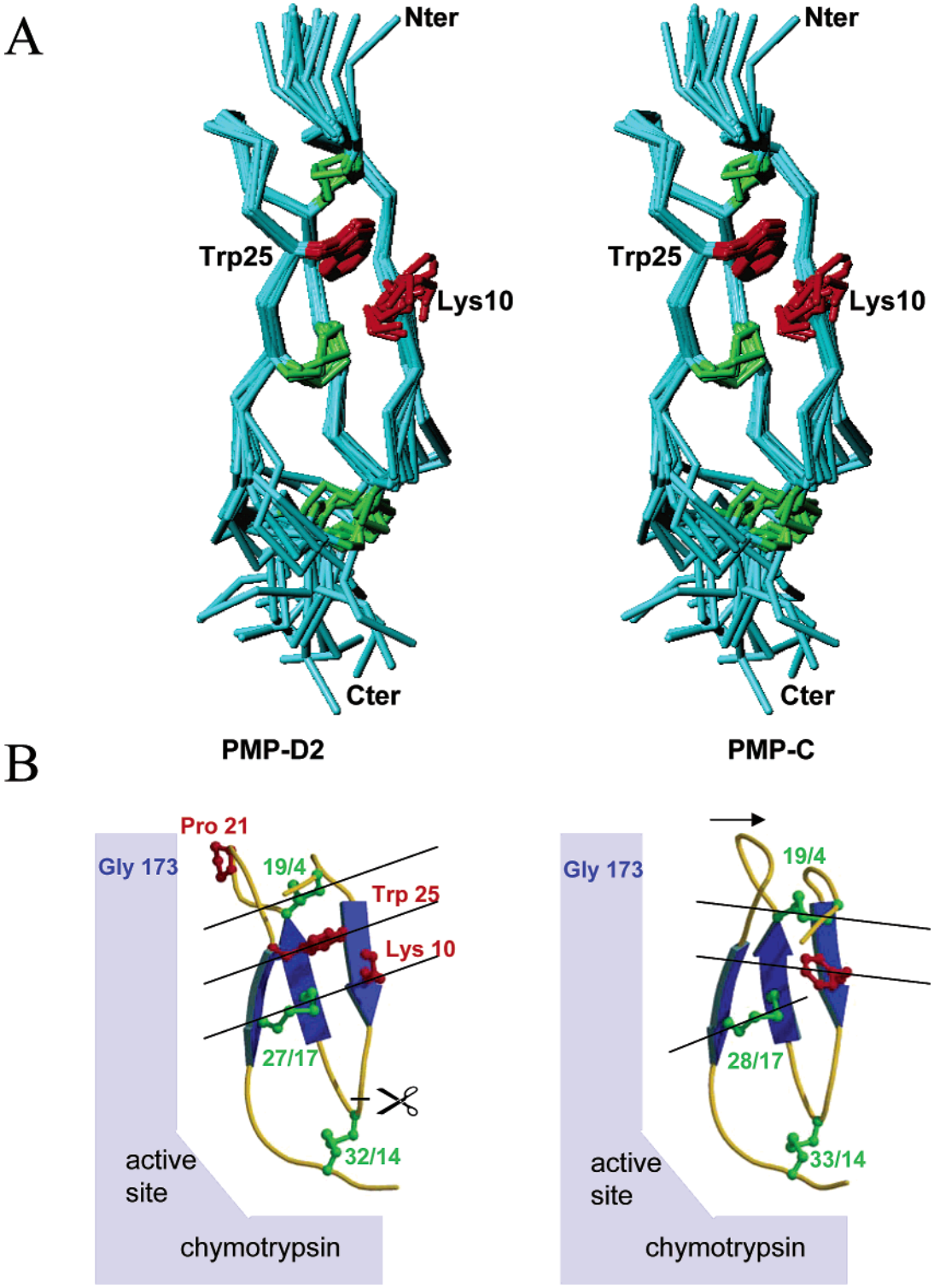

FIGURE 2: NMR structure of HI and comparison with PMP-D2 and PMP-C. (A) Stereo plot of the Cα trace of the 16 final energy-minimized structures of HI. The three disulfide bridges are colored in green. Trp25 and Lys10 that play an important role in the rigidity of the molecule are colored in red. (B) The crystal structures of PMP-D2v and PMP-C in complex with chymotrypsin (schematic drawing) are shown in a similar orientation as HI in part A. The molecules are colored according to the secondary structure (strand in blue, rest in yellow). The three residues mutated in the C-like PMP-D2 analogue are colored in red in PMP-D2v as well as the single aromatic residue in PMP-C.

inhibitor of locust trypsin TRY1 with a K_i = 2 nM (Supporting Information, Figure 2C), while it is known as a highly potent inhibitor of bovine trypsin (from literature, K_i = 0.01−0.5 pM).

Experiments with BApNa as a substrate demonstrate that PMP-D2, HI, and BPTI are also potent inhibitors of TRY2A trypsin with $K_i \leq 0.1$ nM. However, in contrast to trypsin TRY1, when low concentrations of more sensitive substrates (S-2444 or S-2222) are used with trypsin TRY2A, the values of initial velocity (v_0) and velocity in the presence of an inhibitor (v) were not reproducible enough to deduce more precisely K_i.

In addition, supplemetary inhibition experiments indicate that PMP-D2 and HI are also potent inhibitors of *Fusarium*

Table 2: Kinetic Constants (K_i, nM) of Locust Inhibitors and Analogues for Trypsins[a]

peptide	bovine	locust TRY1	locust TRY2A	fungal
BPTI	0.0005−0.00001[b]	2.0 ± 0.2	≤0.10 ± 0.01	ND
HI	40 ± 12	≤0.02 ± 0.005[c]	≤0.05 ± 0.01	≤0.026 ± 0.005
PMP-D2	100 ± 30	≤0.02 ± 0.005[c]	≤0.10 ± 0.015	≤0.026 ± 0.005
SGTI[d]	200[d]			
PMP-D2 (13-35)	NI	8.0 ± 2.0	400 ± 100	NI
EcoPMP-D2	NI	0.50 ± 0.03	40 ± 13	ND
C-like PMP-D2	9.2 ± 3.0	0.20 ± 0.05	ND	≤0.13 ± 0.03
SGCI (L30R)[d]	5.5[d]			

[a] NI means no inhibition under our experimental conditions (K_i > 5000 nM). ND means not determined. [b] Vincent and Lazdunski (*25*). [c] Value estimated with S-2222 substrate. [d] Malik et al. (*5*).

oxysporum trypsin with $K_i \leq 0.026$ nM as estimated by the linear inhibition curves.

Evaluation of the Inhibitory Properties of Analogues of Locust Peptides. In the field of cystine-rich peptides or small proteins such as serine protease inhibitors, many efforts are made to shorten them while keeping their active binding loops, as illustrated by ref *20*. But the minimal requirements and the key structural determinants for inhibition still remain under careful investigation (*21*). In this context, the role of the disulfide bonds and of the core scaffold of the locust peptides in their inhibitory power was investigated. We designed analogues and assayed them on various trypsins: mammalian (bovine and porcine trypsin) and nonmammalian, i.e., insect (*L. migratoria*) or fungal (*F. oxysporum*).

Importance of the Disulfide Bonds. The importance of the disulfide bonds was evaluated by two different approaches. At first the necessity of the whole scaffold was assessed. PMP-D2 was simply N-terminally truncated of 12 residues to yield a short analogue (Figure 1B), and Cys19 was replaced by Ala. The resulting peptide is therefore missing the Cys4−Cys19 bond. The refolding process yielded two isomers accounting for native and nonnative disulfide bonds, with one isomer being totally inactive. The active analogue lost some of its inhibitory properties toward locust TRY1 and TRY2A, with $K_i = 8$ nM and 400 nM, respectively (Table 2). Additionally, no activity could be detected toward bovine or fungal trypsins ($K_i > 5$ μM) under our experimental conditions.

In a second instance, we used a structure-based approach. When crystal structures of PMP-D2 were compared with those of other small canonical inhibitors, we found striking similarities with Ecotin (*22*), a "multitask" inhibitor from *Escherichia coli*. PMP-D2 and Ecotin both display an internal segment (residues 11−20 and 47−56, respectively) connected to the reactive loop by a disulfide bond (Cys14−Cys32 and Cys50−Cys87, respectively) and a similar hydrogen-bond network. However, the second disulfide bond (Cys17−Cys27) present in PMP-D2 is missing in Ecotin (His53 and Ser82 instead of the two cysteines). Therefore the analogue PMP-D2(C17H/C27S) (Figure 1B) was designed to explore the importance of the Cys17−Cys27 bond in maintaining the binding loop of the resulting structure for the inhibitory activity. The refolding of this analogue yielded a complex mixture of disulfide bond isomers. Due to the lack of sufficient amount of material, only the major product was purified and assayed. It was a weaker inhibitor of locust trypsin TRY1 than native PMP-D2 with $K_i = 0.5$ nM and it showed a residual activity toward trypsin TRY2A with a $K_i = 40$ nM. No activity toward bovine trypsin could be detected. Although this analogue was not further analyzed, the residual activity may indicate a properly folded peptide.

The loss of one of the disulfide bonds directly involved in maintaining the reactive loop (EcoPMP-D2) is less dramatic than the truncation of the N-terminal part of the molecule for the interaction with the locust enzymes.

Inhibitory Properties of C-like PMP-D2. In a previous report (*9*), we made the hypothesis that the selectivity of PMP-D2 and HI is conferred by the loop lying from residues 20 to 24, which forms the secondary interaction site with chymotrypsin. As shown by the NMR study, this loop is maintained in a rigid conformation by Pro21 and is positioned by Trp25, which bends the molecule (Figure 2B). The hydrophobic interaction between Trp25 and the alkyl part of Lys10 also contributes to firmly lock the conformation. To check this hypothesis, we designed an analogue of PMP-D2 lacking these two structural features. It appeared that an aromatic residue is essential for the integrity of the peptide. Indeed, the refolding of the single variant W25A of PMP-D2 yielded several oxidation products and the major one showed a disordered conformation, as judged by NMR (unpublished results). In PMP-C, the aromatic residue (Phe) is located in position 10, away from the loop 20−24. Therefore, we interchanged these amino acids by mutating Lys10 into Trp and Trp25 into Ala. Finally, to give more flexibility, Pro21 was replaced by Ala. The resulting triple variant K10W/P21A/W25A was named C-like PMP-D2. Its activity toward locust TRY1 and fungal trypsins was decreased ($K_i = 0.2$ nM and ≤ 0.13 nM, respectively) while it was increased toward bovine trypsin by 1 order of magnitude ($K_i = 9.2$ nM). In addition, porcine trypsin became inhibited ($K_i = 5$ μM). Altogether, these data highlight the notable loss of selectivity of C-like PMP-D2, compared to the native peptide.

Circular Dichroism Study. We previously reported the CD spectrum of PMP-D2, which showed an unusual behavior for a β-sheet structure, with a minimum at 200 nm and a positive band at 227 nm. This was attributed to Trp25 in a particular environment, i.e., in strong interaction with Lys10 aliphatic part. The variant C-like PMP-D2 exhibits some differences, the minimum and maximum bands and the *x*-axis intercept are slightly shifted. A more drastic change occurs for PMP-D2(13−35). The broad positive band at 227 nm was abolished while the negative band was unchanged. As a control, a single mutation (T20A) of PMP-D2 does not affect the CD spectrum. Although these data are hardly interpretable, several characteristics can be drawn. The Trp25 in interaction accounts for an important contribution to the shape of the spectrum, as negatively illustrated with the short

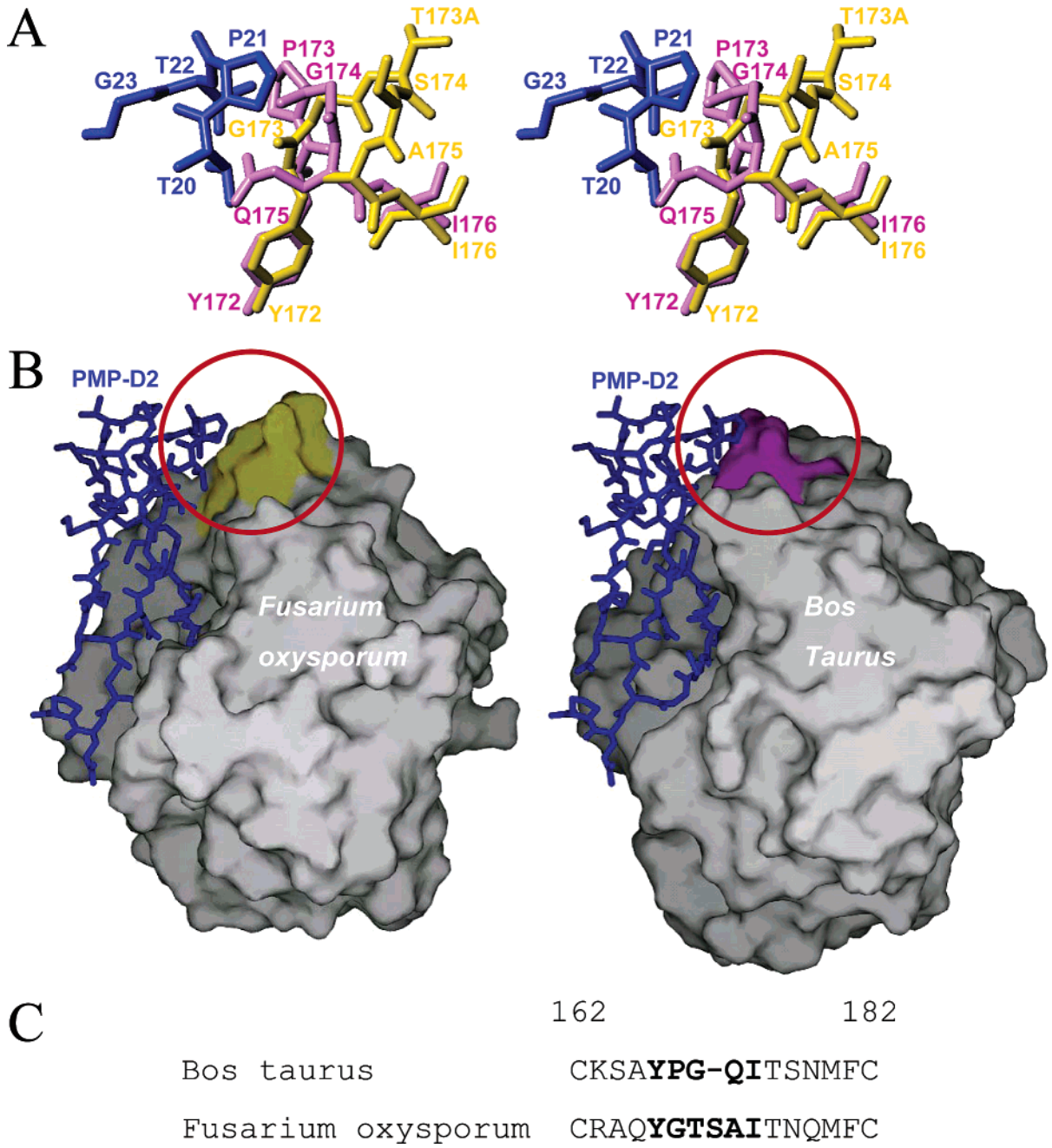

FIGURE 3: Model of PMP-D2 in complex with fungal and bovine trypsins. The complexes between PMP-D2 and fungal or bovine trypsins have been modeled on the basis of the crystal structure of PMP-D2v in complex with bovine chymotrypsin by superposing trypsins onto chymotrypsin. (A) Stereo plot showing the interaction between the region from residue 20 to 23 of the inhibitor (in blue) and the region from residue 172 to 176 of the bovine (in magenta) or fungal (in yellow) trypsin. Pro21 of the inhibitor makes a steric clash with Pro173 of bovine trypsin. (B) Molecular surfaces of the two trypsins are colored in gray except for the loops 172−176 that are colored in yellow (fungal trypsin) and in magenta (bovine trypsin). These loops are situated at the border of the active crevice in which the inhibitor has been modeled. (C) Sequence alignment of region 162−182 in bovine and fungal trypsins.

variant PMP-D2(13−35). In C-like PMP-D2, this particular behavior is restored by the creation of a local environment for Trp25, in the absence of Lys10.

DISCUSSION

Here we report the properties of two peptides PMP-D2 and HI from *L. migratoria* as potent inhibitors of trypsins localized in the digestive tract of the same insect. PMP-D2 and HI are produced by many organs, in particular the fat body but not the midgut (*23*), and are also found in the hemolymph (*4*). Their differential activity toward several trypsins (porcine, bovine, locust, and fungal) clearly points out the high degree of selectivity of these peptides. These results are in accordance with the properties of SGTI from *S. gregaria*. This peptide is a poor bovine trypsin inhibitor and interacts strongly with arthropod (crayfish *Astacus fluviatilis* and shrimp *Penaeus monodon*) trypsins (*24*). All these data may indicate a possible role in the protection from damages caused by protease leakage in the insect. These may also suggest that the more advanced trypsins of mammals diverged from insect/arthropod proteases, perhaps to escape from inhibitors present in their meal.

As previously described, chymotrypsin inhibitors PMP-C and SGCI do not display such a discrimination in their

inhibition pattern. Therefore, the reasons for PMP-D2 and HI selectivity were investigated by comparing PMP-D2v to PMP-C, by use of their structures in complex with bovine α-chymotrypsin. They reveal a main difference in the orientation of the loop 20−24. In the NMR structure of HI (Figure 2A), this loop is well-defined and stands in a conformation superimposable to that of PMP-D2v crystal structure. Its role in the inhibitory properties of PMP-D2 was explored by designing the analogue C-like PMP-D2. Mutations outside of the reactive loop (K10W, P21A, W25A) produce an increased activity toward bovine and porcine trypsins and thus a partial loss of selectivity.

We have modeled PMP-D2 and HI in interactions with various trypsins based on the crystal structure of PMP-D2v in complex with chymotrypsin. This was made possible due to the rigidity of HI, as demonstrated by the NMR study. The docking of PMP-D2 and HI to bovine trypsin results in a steric clash between the loop 20−24 and Pro 173 of the enzyme (Figure 3A,B). This could explain their weak activity toward this protease. In all the chymotrypsins found in the MEROPS database (http://merops.sanger.ac.uk), the corresponding residue is a glycine (Gly173). The position 173 is located on a small loop between the fifth and sixth strands that displays a highly conserved sequence in mammalian trypsins (MEROPS database). On the contrary, insect, arthropod, and fungal trypsins display a larger loop devoid of proline (Figure 3C). The docking of PMP-D2 and HI to *F. oxysporum* trypsin (PDB 1TRY) indicates a favorable interaction with no obvious steric hindrance. Our model is validated by the experimental data in which PMP-D2 and HI appear as potent inhibitors of the fungal trypsin ($K_i \leq$ 0.026 nM). We thus propose the residue 173 to be one of the key determinants in governing inhibitory properties of PMP-D2 and HI (and SGTI).

Trypsin-like proteases are involved in many important biological processes such as digestion, defense, development, and blood coagulation. Natural peptidic inhibitors from many different sources have been studied in order to better understand their regulation. Invertebrates have already been demonstrated to be truly useful models in this domain. In this context, PMP-D2 and HI open a novel field of investigation for engineering their natural selectivity toward targets of therapeutic or agronomical interest.

ACKNOWLEDGMENT

We gratefully acknowledge Dr. W. Lam (previously at Birbeck College, U.K.) for preparing samples of trypsins from *L. migratoria* and Dr. W. Rypniewski (Institute of Bioorganic Chemistry, Poznan, Poland) and Novozymes A/S for providing us *F. oxysporum* trypsin. We thank Dr C. Cambillau (AFMB, Marseille, France) for his constant interest and support.

SUPPORTING INFORMATION AVAILABLE

Two figures, showing the nOe and RMSD distribution versus the sequence of the NMR structure of HI and typical curves of kinetics of inhibition of locust trypsin. This material is available free of charge via the Internet at http://pubs.acs.org.

REFERENCES

1. Schechter, I., and Berger, A. (1967) On the size of the active site in proteases. I. Papain, *Biochem. Biophys. Res. Commun. 27*, 157−62.
2. Laskowski, M. J., and Qasim, M. A. (2000) What can the structures of enzyme−inhibitor complexes tell us about the structures of enzymes substrate complexes? *Biochim. Biophys. Acta 1477*, 324−337.
3. Polanowski, A., Wilusz, T., Blum, M. S., Escoubas, P., Schmidt, J. O., and Travis, J. (1992) Serine proteinase inhibitor profiles in the hemolymph of a wide range of insect species, *Comp. Biochem. Physiol. 102B*, 757−760.
4. Kellenberger, C., Boudier, C., Bermudez, I., Bieth, J. G., Luu, B., and Hietter, H. (1995) Serine protease inhibition by insect peptide containing a cysteine-knot and a triple-stranded β-sheet, *J. Biol. Chem. 270*, 25514−25519.
5. Malik, Z., Amir, S., Pál, G., Buzás, Z., Várallyay, E., Antal, J., Szilágyi, Z., Vékey, K., Asbóth, B., Patthy, A., and Gráf, L. (1999) Proteinase inhibitors from desert locust *Schistocerca gregaria*: engineering both P1 and P1′ residues converts a potent chymotrypsin inhibitor to a potent trypsin inhibitor, *Biochim. Biophys. Acta 1434*, 143−150.
6. Mer, G., Kellenberger, C., Koehl, P., Stote, R., Sorokine, O., Van Dorsselaer, A., Luu, B., Hietter, H., and Lefèvre, J.-F. (1994) Solution structure of PMP-D2, a 35-residue peptide isolated from the insect *Locusta migratoria*, *Biochemistry 33*, 15397−15407.
7. Mer, G., Kellenberger, C., Renatus, M., Luu, B., Hietter, H., and Lefèvre, J.-F. (1996) Solution structure of PMP-C: a new fold in the group of small proteinase inhibitors, *J. Mol. Biol. 258*, 158−171.
8. Gaspari, Z., Patthy, A., Graf, L., and Perczel, A. (2002) Comparative structure analysis of proteinase inhibitors from the desert locust, *Schistocerca gregaria*, *Eur. J. Biochem. 269*, 527−37.
9. Roussel, A., Mathieu, M., Dobbs, A., Luu, B., Cambillau, C., and Kellenberger, C. (2001) Complexation of two proteic insect inhibitors to chymotrypsin's active site suggests decoupled roles for binding and selectivity, *J. Biol. Chem. 276*, 38893−38898.
10. Katz, B. A., Sprengeler, P. A., Luong, C., Verner, E., Elrod, K., Kirtley, M., Janc, J., Spencer, J. R., Breitenbucher, J. G., Hui, H., McGee, D., Allen, D., Martelli, A., and Mackman, R. L. (2001) Engineering inhibitors highly selective for the S1 sites of Ser190 trypsin-like serine protease drug targets, *Chem. Biol. 8*, 1107−21.
11. Bieth, J. G. (1995) Theoretical and practical aspects of proteinase inhibition kinetics, *Methods Enzymol. 248*, 59−84.
12. Bartels, C., Xia, T., Billeter, M., Guntert, P., and Wuthrich, K. (1995) The program XEASY for computer-supported NMR spectral analysis of biological macromolecules, *J. Biomol. NMR 5*, 1−10.
13. Wuthrich, K. (1986) *NMR of Proteins and Nucleic Acids*, Wiley, New York.
14. Guntert, P., and Wuthrich, K. (1991) Improved efficiency of protein structure calculations from NMR data using the program DIANA with redundant dihedral angle constraints, *J. Biomol. NMR 1*, 447−56.
15. Bernard, C., Corzo, G., Mosbah, A., Nakajima, T., and Darbon, H. (2001) Solution structure of Ptu1, a toxin from the assassin bug *Peirates turpis* that blocks the voltage-sensitive calcium channel N-type, *Biochemistry 40*, 12795−800.
16. Roussel, A., and Cambillau, C. (1991) in *Silicon Graphics Geometry Parterns Directory*, p 86, Silicon Graphics, Mountain View, CA.
17. Laskowski, R. A., Rullmannn, J. A., MacArthur, M. W., Kaptein, R., and Thornton, J. M. (1996) AQUA and PROCHECK-NMR: programs for checking the quality of protein structures solved by NMR, *J. Biomol. NMR 8*, 477−86.
18. Mer, G., Dejeagere, A., Stote, R., Kieffer, B., and Lefèvre, J. F. (1996) Structural dynamics of PMP-D2: an experimental and theorical study, *J. Phys. Chem. 100*, 2667−2674.
19. Lam, W., Coast, G. M., and Rayne, R. C. (2000) Characterisation of multiple trypsins from the midgut of *Locusta migratoria*, *Insect Biochem. Mol. Biol. 30*, 85−94.
20. McBride, J. D., Freeman, H. N., and Leatherbarrow, R. J. (1999) Selection of human elastase inhibitors from a conformationally constrained combinatorial peptide library, *Eur. J. Biochem. 266*, 403−12.
21. Radisky, E. S., King, D. S., Kwan, G., and Koshland, D. E., Jr. (2003) The role of the protein core in the inhibitory power of the

classic serine protease inhibitor, chymotrypsin inhibitor 2, *Biochemistry 42*, 6484−92.
22. McGrath, M. E., Erpel, T., Bystroff, C., and Fletterick, R. (1994) Macromomecular chelation as an improved mechanism of protease inhibition: structure of the ecotin−trypsin complex. *EMBO J. 13*, 1502−1507.
23. Kromer, E., Nakakura, N., and Lagueux, M. (1994) Cloning of a *Locusta* cDNA encoding a precursor peptide for two structurally related proteinase inhibitors. *Insect Biochem. Mol. Biol. 24*, 329−331.
24. Patthy, A., Amir, S., Malik, Z., Bodi, A., Kardos, J., Asboth, B., and Graf, L. (2002) Remarkable phylum selectivity of a *Schistocerca gregaria* trypsin inhibitor: the possible role of enzyme−inhibitor flexibility, *Arch Biochem. Biophys. 398*, 179−87.
25. Vincent, J. P., and Lazdunski, M. (1972) Trypsin−pancreatic trypsin inhibitor association. Dynamics of the interaction and role of disulfide bridges, *Biochemistry 11*, 2967−2977.

BI035318T